

the correlation between $F(t)$ and C_p when the linear effect of C was removed from $F(t)$ and C_p . This measure is useful, because an IT neuron has a tendency to encode both of the paired stimuli ("pair-coding" effect) (18, 25, 34) and because this correlation between C and C_p must be removed in the multiple regression analysis of $F(t)$. Neural discharges of IT cells reflect the cognitive demand of the PA task, and stimulus-selective delay activities are closely coupled with a strong cue response to its paired associate. This property of the delay discharges is now known as "target-related" or "prospective" signals (18, 19, 25). $PRI(t)$ is influenced by weak responses if the stimulus selectivity of the neuron is rather broad, but not heavily if the stimulus selectivity is sharp, as in the case of the neuron shown in Fig. 2. $PRI(t)$ s were fitted with cumulative Weibull functions [see text and (29)] by using the data stepped by 5 ms as stated above; however, for convenience, the data were plotted every 40 ms in Fig. 2, C and F, and plotted every 100 ms in Fig. 2, G and H.

24. J. A. Movshon, W. T. Newsome, *J. Neurosci.* **16**, 7733 (1996).
25. C. A. Erickson, R. Desimone, *J. Neurosci.* **19**, 10404 (1999).
26. The stimulus selectivity during the cue period (60 to 320 ms from cue onset) and the delay period (1320 to 2320 ms from cue onset) was tested by a one-way ANOVA ($P < 0.01$). All the delay-selective neurons were also cue-selective in both A36 and TE. The numbers of selective cells were 40 (TE) and 32 (A36) in monkey 1, 15 (TE) and 8 (A36) in monkey 2, and 14 (TE) and 5 (A36) in monkey 3. The proportion of delay-selective neurons in relation to cue-selective neurons (A36, 45/97; TE, 69/321) was significantly higher in A36 than in TE (χ^2 test, $df = 1$, $P < 0.001$).
27. Spike trains were smoothed by convolution with a Gaussian kernel ($\sigma = 10$ ms) to obtain the spike density function (SDF). The baseline activity was defined as the mean discharge rate during the 300-ms period just preceding cue onset. The latency of the neuronal response was determined as the time point when the SDF for the optimal stimulus first exceeded a level +2 standard deviations from the baseline activity.
28. A repeated-measures ANOVA (Area \times Time \times Animal) was used to compare the time courses of $PRI(t)$ for the population of stimulus-selective neurons (subject factor; neurons, $df = 108$) in each area (between-subject factor; Area, $df = 1$) of each animal (between-subject factor; Animal, $df = 2$) at each time point ($t = 0, 100, \dots, 2300$ ms) (within-subject factor; Time, $df = 23$). The interaction between Area and Time indicated significant difference in the time course between the two areas ($P < 0.0001$). There was neither a main effect of Animal ($P > 0.12$) nor an interaction among Area, Time, and Animal ($P > 0.084$). The time course of the $PRI(t)$ in each animal was also examined by a repeated-measures ANOVA (Area \times Time). The interactions between Area and Time were significant in all the animals ($P < 0.0001$, $P < 0.002$, $P < 0.0001$, respectively).
29. To characterize the growth in $PRI(t)$ with time, we fitted the data with a cumulative Weibull function (30, 31)

$$W(t) = \gamma - (\gamma - \delta) \cdot \exp[-(t/\alpha)^\beta]$$

where γ is the maximum value, δ is the minimum value, t is the time after cue presentation, α is the time point at which the curve reaches 64% of its full growth, and β is the slope in the PRI . The best-fit Weibull function was determined by using the data after cue onset. Among the 114 stimulus-selective neurons, TRT and TRD were determined for the stimulus-selective neurons whose best-fit Weibull function for the $PRI(t)$ increased above the 5% significance level ($r = 0.352$, $df = 21$). The best-fit Weibull curves accurately represented the PRI change with time for these neurons as judged by the R^2 values ($R^2 = 0.35$ to 0.95 , mean 0.66).

30. S. Celebiri, W. T. Newsome, *J. Neurosci.* **14**, 4109 (1994).
31. K. G. Thompson *et al.*, *J. Neurophysiol.* **76**, 4040 (1996).
32. A two-way ANOVA was used to evaluate effects of Area and Animal on the TRT and TRD values. There

was a significant main effect of Area ($P < 0.008$), indicating difference in the TRT values between A36 and TE. Neither a main effect of Animal ($P > 0.8$) nor an interaction between Area and Animal ($P > 0.35$) were significant, which assured across-animal consistency in the TRT values. In the case of TRD, there were neither main effects (Area, $P > 0.75$; Animal, $P > 0.70$) nor an interaction ($P > 0.23$).

33. D. J. Amit, N. Brunel, M. V. Tsodyks, *J. Neurosci.* **14**, 6435 (1994).
34. S. Higuchi, Y. Miyashita, *Proc. Natl. Acad. Sci. U.S.A.* **93**, 739 (1996).
35. E. A. Buffalo *et al.*, *Learn. Mem.* **6**, 572 (1999).
36. M. J. Buckley, D. Gaffan, E. A. Murray, *J. Neurophysiol.* **77**, 587 (1997).

37. H. Tomita *et al.*, *Nature* **401**, 699 (1999).
38. I. Hasegawa *et al.*, *Science* **281**, 814 (1998).
39. Experiments were conducted in accordance with the NIH Guide for the Care and Use of Laboratory Animals and with the regulations of the National Institute for Physiological Sciences, Japan. This work was supported by a Grant-in-Aid for Specially Promoted Research (07102006) to Y.M. and by a Grant-in-Aid for Encouragement of Young Scientists (09780744) to Y.N. from the Japanese Ministry of Education, Science, Sports and Culture. We thank A. Ito and S. Shibata for technical assistance and T. Isa, H. Komatsu, S. Mori, K. Ohki, and H. Okuno for discussions.

15 August 2000; accepted 18 December 2000

Glycolipid Antigen Processing for Presentation by CD1d Molecules

Theodore I. Prigozy,¹ Olga Naidenko,¹ Pankaj Qasba,² Dirk Elewaut,¹ Laurent Brossay,^{1*} Archana Khurana,¹ Takenori Natori,³ Yasuhiko Koezuka,³ Ashok Kulkarni,⁴ Mitchell Kronenberg^{1†}

The requirement for processing glycolipid antigens in T cell recognition was examined with mouse CD1d-mediated responses to glycosphingolipids (GSLs). Although some disaccharide GSL antigens can be recognized without processing, the responses to three other antigens, including the disaccharide GSL Gal($\alpha 1 \rightarrow 2$)GalCer (Gal, galactose; GalCer, galactosylceramide), required removal of the terminal sugars to permit interaction with the T cell receptor. A lysosomal enzyme, α -galactosidase A, was responsible for the processing of Gal($\alpha 1 \rightarrow 2$)GalCer to generate the antigenic monosaccharide epitope. These data demonstrate a carbohydrate antigen processing system analogous to that used for peptides and an ability of T cells to recognize processed fragments of complex glycolipids.

T cells typically recognize peptide antigens presented by major histocompatibility complex-encoded class I or class II molecules. These peptides are generated from well-characterized pathways of protein antigen processing (1, 2). T cells that recognize microbial glycolipids in the context of CD1 molecules play a role in host defense (3, 4). Additionally, many T cells are reactive with autologous lipids presented by CD1 molecules (5, 6). These cells could be important for regulating immune responses and preventing autoimmune disease (7). Despite the

significance of this antigen recognition system, there is little information on the transport and generation of glycolipids for CD1 presentation.

To determine if carbohydrates can be processed for antigen presentation, we investigated the CD1d-mediated recognition of glycosphingolipids (GSLs). α -Galactosylceramide (α -GalCer) (Fig. 1A) is a GSL isolated from a marine sponge in a screen for anti-metastatic compounds (8). It is distinguished from other natural GSLs by the α anomeric linkage of the sugar to the lipid. The cells that respond to α -GalCer presented by CD1d are a separate T cell lineage known as natural killer (NK) T cells (9, 10).

We analyzed the response to two closely related α -GalCer analogs, Gal($\alpha 1 \rightarrow 2$)Gal($\alpha 1 \rightarrow 1$)Cer [or Gal($\alpha 1 \rightarrow 2$)GalCer] and Gal($\alpha 1 \rightarrow 6$)GalCer (Fig. 1A). An antigen-presenting cell (APC)-free T cell stimulation assay was used to test the possibility that presentation of these antigens requires internalization and processing (11, 12). Although α -GalCer and Gal($\alpha 1 \rightarrow 6$)GalCer bound to mouse CD1d-coated plates could stimulate interleukin-2 (IL-2) release by NK T cell hybridomas, Gal($\alpha 1 \rightarrow 2$)GalCer could not (Fig. 1B). This

¹Division of Developmental Immunology, La Jolla Institute for Allergy and Immunology, 10355 Science Center Drive, San Diego, CA 92121, USA. ²Developmental and Metabolic Neurology Branch, National Institute of Neurological Disorders and Stroke, National Institutes of Health, Bethesda, MD 20892, USA. ³Pharmaceutical Research Laboratory, Kirin Brewery, Gunma 370-12, Japan. ⁴Functional Genomics Unit, National Institute of Dental and Craniofacial Research, Bethesda, MD 20892, USA.

*Present address: Department of Molecular Microbiology and Immunology, Brown University, Providence, RI 02912, USA.

†To whom correspondence should be addressed. E-mail: mitch@liai.org

did not reflect a requirement for low pH to allow antigen loading of CD1d, because incubation of CD1d with Gal(α 1 \rightarrow 2)GalCer at mildly acidic pH also did not permit a T cell response.

CD1b molecules require entry into late endosomal compartments to present mycobacterial lipid antigens (13, 14). In contrast, CD1d molecules lacking the endosomal targeting motif YQDI (Y, Tyr; Q, Gln; D, Asp; I, Ile) can present α -GalCer to NK T cells (10). Further, Gal(α 1 \rightarrow 2)GalCer can stimulate NK T cell responses in the presence of CD1d⁺ APCs (9). To determine if presentation of Gal(α 1 \rightarrow 2)GalCer requires trafficking of CD1d to putative antigen processing compartments, we transfected A20 B lymphoma cells with CD1d or with a cytoplasmic tail-deleted CD1d (CD1d/TD) lacking the YQDI sorting motif required for routing to endosomes. APCs were pulsed with pepstatin labeled with Bodipy FL (Molecular Probes, Eu-

gene, Oregon) to detect lysosomes, and after fixation, CD1d molecules were immunolocalized (Fig. 2A). Wild-type CD1d molecules colocalized with labeled pepstatin (Fig. 2A, left), indicating their presence in lysosomes (Fig. 2A, white arrows), as well as on the plasma membrane. In the A20 CD1d/TD cells (Fig. 2A, right), most CD1d molecules were on the cell surface, and pepstatin-containing vesicles were largely devoid of CD1d labeling. Using a standard antigen presentation assay (15), we found that Gal(α 1 \rightarrow 2)GalCer was antigenic for NK T cell hybridomas when incubated with APCs expressing wild-type CD1d, but not when incubated with the CD1d/TD mutation (Fig. 2B). By contrast, the presentation of both α -GalCer and Gal(α 1 \rightarrow 6)GalCer was insensitive to the YQDI deletion.

We also measured the impact of lysosomotropic inhibitors on GSL antigen presentation (Fig. 2C). Concanamycin A (CMA), an inhibitor of the vacuolar adenosine triphosphatase/H⁺ pump, completely blocked presentation of Gal(α 1 \rightarrow 2)GalCer but only mildly inhibited the other GSLs. Bafilomycin A1 (Baf), which interferes with the uptake of macromolecules (16), reduced the presentation of Gal(α 1 \rightarrow 2)GalCer by fourfold, with no effect on the other GSLs (Fig. 2C). However, when the APCs were

pulsed with antigen before the addition of Baf, the reduction in Gal(α 1 \rightarrow 2)GalCer presentation was reversed, consistent with an effect on antigen internalization (17).

To characterize the processing of Gal(α 1 \rightarrow 2)GalCer, we focused on the lysosomal enzyme α -galactosidase A (α -Gal A) (18), which should catalyze the removal of the terminal galactose. Deoxygalactonojirimycin (DGJ) is a potent and selective inhibitor of α -galactosidase activity (19). Treatment of A20 CD1d transfectants with DGJ eliminated presentation of Gal(α 1 \rightarrow 2)GalCer but not the response to the related glycolipids (Fig. 3A). A control β -galactosidase inhibitor, calystegine C1 (CYN-C1) (20), had no effect (Fig. 3A).

α -Galactosidase from green coffee beans (21), which has properties similar to the mammalian enzyme, was tested to determine if it could process Gal(α 1 \rightarrow 2)GalCer in vitro. The glycolipid was treated with α -galactosidase and added to transfectants expressing CD1d/TD molecules that cannot localize to lysosomes. There was an α -galactosidase-dependent increase in IL-2 production stimulated by Gal(α 1 \rightarrow 2)GalCer (Fig. 3B). The inhibitor DGJ reversed the α -galactosidase-mediated increase (Fig. 3B), demonstrating that this enzyme is necessary and sufficient for in vitro processing

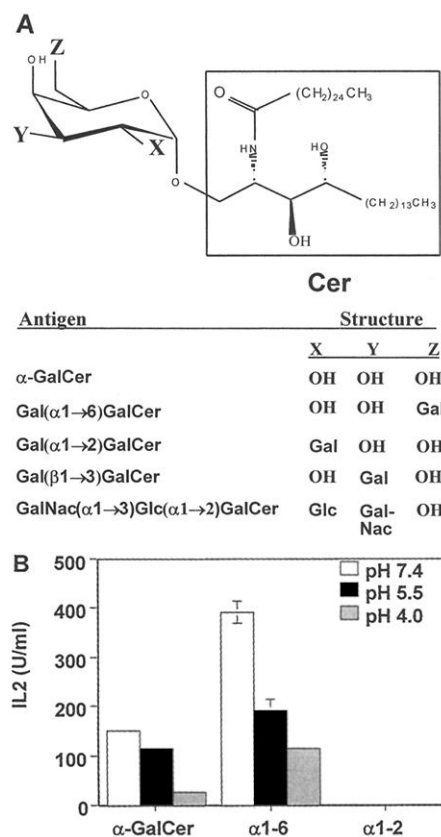


Fig. 1. APC-free recognition of GSLs. (A) Glycolipid structures. X, Y, and Z represent the 2', 3', and 6' positions on the primary galactose of the glycolipids, respectively. (B) Complexes of soluble mouse CD1d and α -GalCer, Gal(α 1 \rightarrow 6)GalCer (designated as α 1-6), or Gal(α 1 \rightarrow 2)GalCer (designated as α 1-2) were used to stimulate the 3C3 NK T cell hybridoma. Soluble CD1d protein was incubated with each glycolipid at different pH values before neutralization and before the wells were coated (12). With each data point, the SEM is shown as an error bar. Similar results were obtained in four independent experiments and with the 1-2 hybridoma as well.

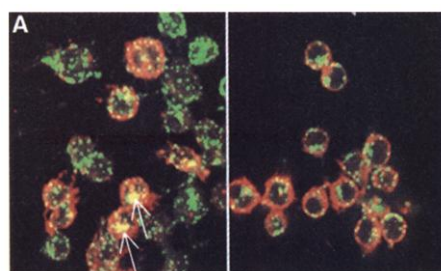
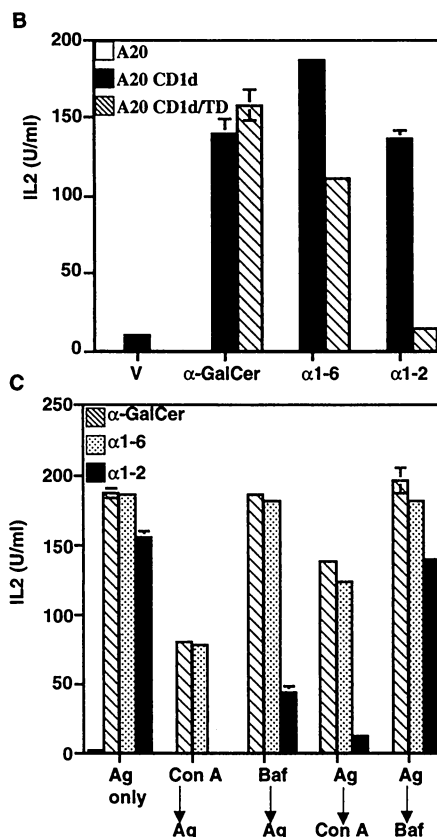
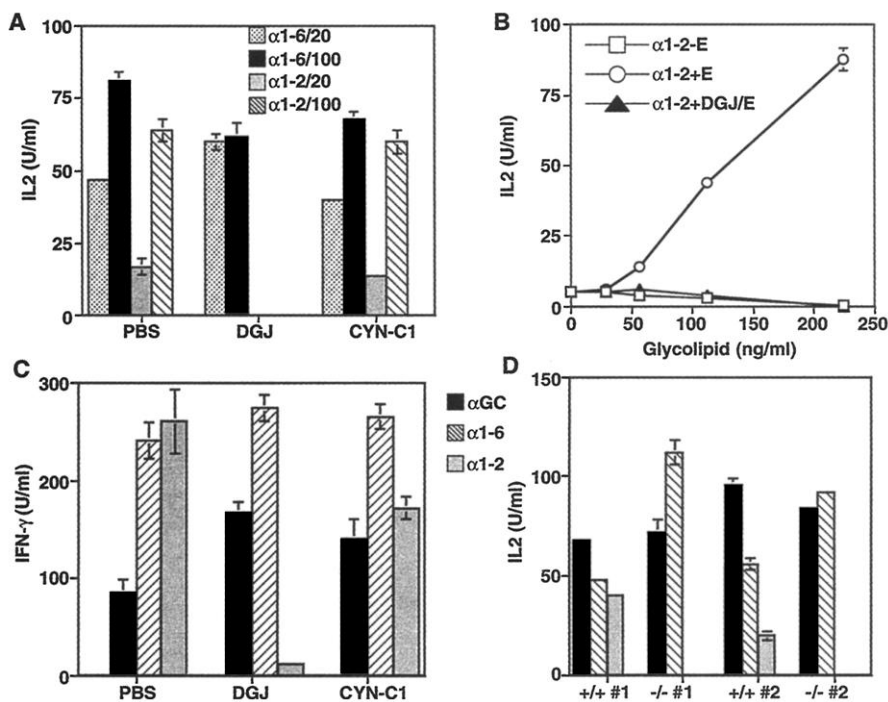


Fig. 2. Requirement of lysosomes for GSL recognition. (A) A20 transfectants expressing wild-type CD1d (A20 CD1d, left) or tail-deleted CD1d (A20 CD1d/TD, right) were pulsed for 2 hours with pepstatin labeled with Bodipy FL, indicating lysosomes (green). After fixation, CD1d molecules were immunofluorescently labeled (37). The colocalization of red (CD1d) and green fluorescence is depicted by a yellow signal. The white arrows in (A) indicate lysosomes containing CD1d and pepstatin. (B) A20 CD1d or A20 CD1d/TD cells were pulsed for 3 hours with either the vehicle DMSO (V) or the indicated antigens (15). Shown is the antigen-dependent IL-2 production by the 3C3 hybridoma for A20, A20 CD1d, and A20 CD1d/TD. (C) Blockade of Gal(α 1 \rightarrow 2)GalCer presentation by lysosomotropic agents. APCs (A20 CD1d) were treated with the indicated antigen (Ag) alone, with 10 nM CMA, or with 50 nM Baf for 5 min before the addition of antigens or for 3 hours with antigen followed by an additional 1-hour incubation with inhibitor. In both cases, the total time of the antigen pulse was 4 hours (15). Shown are the responses of the 3C3 hybridoma to the vehicle DMSO (missing bars indicate responses that were not visible), and the indicated antigens. In (B) and (C), similar results were obtained in at least three independent experiments with 3C3 and in experiments with the other hybridomas tested; error bars indicate the SEM. α 1-6, Gal(α 1 \rightarrow 6)GalCer; α 1-2, Gal(α 1 \rightarrow 2)GalCer.



REPORTS

Fig. 3. Antigen processing of Gal(α 1 \rightarrow 2)GalCer is mediated by α -Gal A. **(A)** Ablation of Gal(α 1 \rightarrow 2)GalCer presentation by an α -galactosidase inhibitor. A20 CD1d APCs were preincubated with PBS, the α -galactosidase inhibitor DGJ, or the β -galactosidase inhibitor CYN-C1 for 1 hour before the addition of the indicated antigens at the specified doses (in ng/ml). Shown are the responses of the 3C3 hybridoma to the vehicle DMSO (missing bars indicate responses that were not visible) and the two doses of the Gal(α 1 \rightarrow 6) and Gal(α 1 \rightarrow 2) antigens. **(B)** In vitro antigen processing by α -galactosidase. Gal(α 1 \rightarrow 2)GalCer (900 ng) was digested with 2 units of α -galactosidase (E, enzyme) from green coffee beans (Calbiochem, San Diego, CA), in the presence or absence of 1 mM DGJ for 12 hours in citrate-phosphate buffer, pH 5.0. The pH was neutralized for a dose-response antigen presentation assay with 3C3 hybridoma cells and A20 CD1d/TD APCs. In **(A)** and **(B)**, similar results were obtained in four independent experiments with the three NK T cell hybridomas; error bars indicate the SEM. **(C)** Total splenocytes pooled from eight C57BL/6 strain mice (2.5×10^6 cells/well in triplicate) were incubated with PBS, DGJ, or CYN-C1 for 2 hours before the addition of the indicated glycolipids. After 60 hours, the interferon- γ (IFN- γ) production was measured by ELISA. The values shown are the mean of three sets of triplicates with the SEM (error bars). Similar results were also obtained by measuring IL-4 production (32), and the data shown are representative of three independent experiments. **(D)** APCs from α -Gal A $^{-/-}$ mice cannot present Gal(α 1 \rightarrow 2)GalCer. Splenocytes from α -Gal A $^{-/-}$ mice and littermate controls were isolated and pulsed with the indicated antigens. There was no detectable response to the vehicle DMSO. After five washes, 2.5×10^5 irradiated splenocytes per



well were used to stimulate NK T cell hybridomas (1×10^5 cells/well). The data shown are from two individual wild-type and α -Gal A $^{-/-}$ mice; error bars indicate the SEM. Similar results were obtained with the 1-2 hybridoma and in replicate experiments with three different sets of mice. The bar key is the same for **(C)** and **(D)**: α GC, α -GalCer; α 1-6, Gal(α 1 \rightarrow 6)GalCer; α 1-2, Gal(α 1 \rightarrow 2)GalCer.

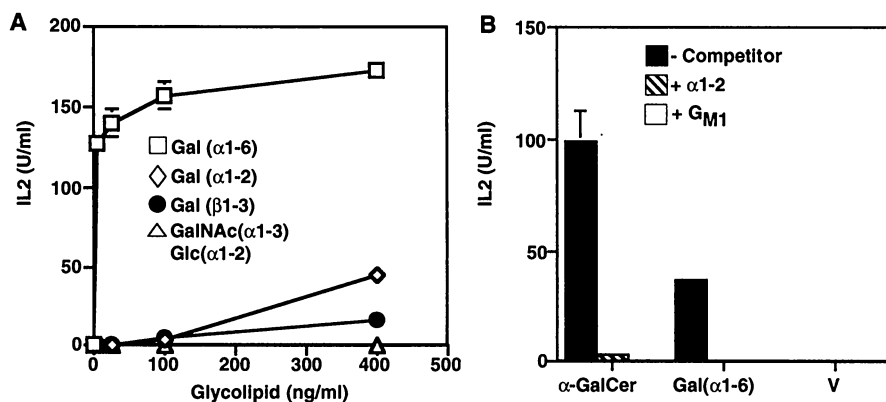


Fig. 4. **(A)** Antigen presentation of four α -GalCer analogs by A20 CD1d/TD APCs. The APCs were pulsed with DMSO or with doses of the antigens depicted. After the antigen pulse, the cells were washed with media before the addition of the hybridoma cells and before IL-2 measurements. The error bars indicate the SEM of triplicate measurements. Representative data from one of three experiments with 3C3 are shown; similar results were obtained with the other hybridomas. **(B)** Gal(α 1 \rightarrow 2)GalCer inhibits antigen presentation by soluble CD1d molecules. Competition binding assays were performed as described (12) with the indicated competitor ligands. Shown is the response of the hybridoma to the indicated glycolipids or the vehicle (V); error bars indicate the SEM (missing bars indicate responses that were not visible). In **(A)** and **(B)**, representative data from one of three experiments with 3C3 are shown, and similar results were obtained with hybridoma 1-2.

(Fig. 3B). Therefore, in vitro processing of Gal(α 1 \rightarrow 2)GalCer by coffee bean α -galactosidase may mimic antigen processing in APCs.

To define the relevance of this pathway for normal lymphocytes, assays were performed on total splenocytes. The addition of GSLs to mouse splenocytes results in the production of cytokines (Fig. 3C), due to

presentation by endogenous APCs to splenic NK T cells (10). DGJ reduced presentation of Gal(α 1 \rightarrow 2)GalCer by spleen cells nearly 20-fold but had no effect on the response to the other GSLs (Fig. 3C).

In humans, α -Gal A deficiency causes Fabry's disease (22), characterized by an accumulation of trihexose ceramide in lyso-

somes. A mouse model for Fabry's disease has been generated by targeted disruption of the α -Gal A gene (23). Splenic APCs derived from α -Gal A $^{-/-}$ mice could not present Gal(α 1 \rightarrow 2)GalCer to the hybridomas (Fig. 3D), although the responses to α -GalCer and Gal(α 1 \rightarrow 6)GalCer were not affected. Interestingly, α -Gal A $^{-/-}$ mice have a selective decrease in the number of splenic NK T cells and in their ability to respond to α -GalCer (24). It remains to be determined, however, if this reflects the inability of processing to form a natural ligand required for the development of NK T cells or some other defect.

To test the generality of our findings, we studied the NK T cell response to two other GSLs. The disaccharide Gal(β 1 \rightarrow 3)GalCer and the trisaccharide GalNAc(α 1 \rightarrow 3)[Glc(α 1 \rightarrow 2)]GalCer (GalNAc, *N*-acetylgalactosamine; Glc, glucose) (Fig. 1A) could not be presented by plates coated with soluble CD1d molecules (25). Consistent with this, these compounds were presented minimally by A20 CD1d/TD APCs (Fig. 4A), although they can be presented by wild-type CD1d APCs (9). Thus, the presence of a second carbohydrate linked to the 3' position of the inner galactose impairs recognition to a similar extent as the substitution at the 2' position (Fig. 4A). To determine if the carbohydrate moieties of these antigens are substrates for lysosomal glycosidases, we measured the effect of in vitro digestion with different glycosidases on antigen presentation by A20

CD1d/TD APCs. The data are consistent with the hypothesis that removal of sugars linked to both the 2' and 3' positions of the galactose is required for T cell stimulation (26).

We have shown previously that carbohydrate is not required for GSL binding to CD1d (11), suggesting that carbohydrate processing is required to permit interaction with the T cell receptor. To test this possibility, we carried out competition studies. Soluble CD1d molecules were briefly preincubated with either ganglioside G_{M1}, which was shown previously to compete for binding of α -GalCer (11), or Gal(α 1 \rightarrow 2)GalCer, before the addition of stimulatory glycolipids. Both G_{M1} and Gal(α 1 \rightarrow 2)GalCer were effective as competitors (Fig. 4B), indicating that the additional sugar on Gal(α 1 \rightarrow 2)GalCer does not prevent its binding to CD1d.

Here, we provided a demonstration of a carbohydrate antigen processing pathway. Interestingly, lysosomal hydrolases, previously thought to be solely involved in GSL metabolism (27), are responsible for this function. We confirmed that α -Gal A is located in lysosomes in APCs by assay of subcellular fractions with a chromogenic substrate (28). Therefore, some of the contents of the lysosome must have access to CD1d molecules, consistent with the presence of CD1d in lysosomes demonstrated here.

Carbohydrate antigen processing illustrates the ability of antigen presentation systems to co-opt metabolic pathways that have evolved for different purposes. The ability to process carbohydrate antigens could greatly extend the range of antigens that are presented by CD1 molecules. Furthermore, T cell antigen recognition of glycopeptides presented by classical class I and class II molecules is known (29), and the carbohydrate linkages in glycopeptides also may be subject to the types of processing events described here.

References and Notes

1. K. L. Rock, A. Goldberg, *Annu. Rev. Immunol.* **17**, 739 (1999).
2. J. A. Villadangos, H. L. Ploegh, *Immunity* **12**, 233 (2000).
3. E. M. Beckman *et al.*, *Nature* **372**, 691 (1994).
4. P. A. Sieling *et al.*, *Science* **269**, 227 (1995).
5. J. E. Gumperz *et al.*, *Immunity* **12**, 211 (2000).
6. A. Shamshiev *et al.*, *Immunity* **13**, 255 (2000).
7. A. Bendelac *et al.*, *Annu. Rev. Immunol.* **15**, 535 (1997).
8. T. Natori *et al.*, *Tetrahedron* **50**, 2771 (1994).
9. T. Kawano *et al.*, *Science* **278**, 1626 (1997).
10. N. Burdin *et al.*, *J. Immunol.* **161**, 3271 (1998).
11. O. Naidenko *et al.*, *J. Exp. Med.* **190**, 1069 (1999).
12. Cell-free antigen presentation assays were performed by coating microwells with 1 μ g of soluble CD1d molecules that had been preincubated with antigen. Among the GSL compounds tested, only α -GalCer and Gal(α 1 \rightarrow 6)GalCer were antigenic in this assay. Competition assays were performed by incubating 2 μ g of soluble CD1d protein with a 5-fold molar excess of Gal(α 1 \rightarrow 2)GalCer or a 10-fold molar excess of G_{M1} gangliosides for 5 min at room temperature before the addition of the vehicle [phosphate-buffered saline (PBS) and 0.05% polysorbate], α -GalCer, or Gal(α 1 \rightarrow 6)GalCer for an additional 2-hour incubation at 37°C. The wells

were then rinsed with PBS and cultured with hybridomas.

13. R. M. Jackman *et al.*, *Immunity* **8**, 341 (1998).
14. V. Briken *et al.*, *J. Exp. Med.* **192**, 281 (2000).
15. APCs were incubated with antigens or the vehicle [dimethyl sulfoxide (DMSO)] for 3 hours at an antigen dose of 50 ng/ml, unless stated otherwise. The antigen-pulsed APCs were washed and plated in 96-well plates in triplicates (1×10^5 cells/well). The responder cells (5×10^4 cells/well) used for each assay were the NK T cell hybridomas 3C3, 1-2, and 1-4 (30), all of which have the invariant V α 14-J α 281 rearrangement characteristic of NK T cells. Antigen-dependent IL-2 production was measured after 16 hours of stimulation by enzyme-linked immunosorbent assay (ELISA).
16. M. Harata *et al.*, *Liver* **17**, 244 (1997).
17. When APCs were pulsed with glycolipids before the addition of CMA, there was only a slight increase in presentation of Gal(α 1 \rightarrow 2)GalCer relative to when CMA is added first. However, α -GalCer and Gal(α 1 \rightarrow 6)GalCer were presented at nearly the same level as the control (antigen only) when they were added before CMA, demonstrating that the more potent CMA can block antigen uptake and lysosome function.
18. A. J. Lusis, K. Paigen, *Biochim. Biophys. Acta* **437**, 487 (1976).
19. N. Asano *et al.*, *Med. Chem.* **37**, 3701 (1994).
20. N. Asano *et al.*, *Eur. J. Biochem.* **248**, 296 (1997).
21. F. Yagi *et al.*, *Arch. Biochem. Biophys.* **280**, 61 (1990).
22. R. O. Brady *et al.*, *N. Engl. J. Med.* **276**, 1163 (1967).
23. T. Ohshima *et al.*, *Proc. Natl. Acad. Sci. U.S.A.* **94**, 2540 (1997).
24. In preliminary studies, a CD1d/ α -GalCer tetramer-based analysis of splenocytes in α -Gal A^{-/-} mice revealed a 50% reduction in NK T cells. This reduction in number was associated with a sixfold reduction in the amount of α -GalCer-dependent IL-4 production by α -Gal A^{-/-} splenocytes relative to wild-type splenocytes.
25. In three independent experiments, these GSLs were not antigenic when used as ligands with CD1d-coated plates to stimulate the 1-2 and 3C3 hybridomas (12).
26. Supplementary material is available at www.sciencemag.org/cgi/content/full/291/5504/664/DC1.
27. K. Sandhoff, T. Kolter, *Trends Cell Biol.* **6**, 98 (1996).
28. Lysosomes from A20 cells were isolated by ultracentrifugation of a light mitochondrial fraction containing 20% Optiprep (iodixanol) according to the manufacturer's instructions (Accurate Chemical, San Diego, CA). The lysosomes were sonicated and spectrophotometrically assayed for α -Gal A activity with *p*-nitrophenyl- α -D-galactoside.
29. A. Glithero *et al.*, *Immunity* **10**, 63 (1999).
30. L. Brossay *et al.*, *J. Immunol.* **160**, 3681 (1998).
31. Cells were fixed, permeabilized, and incubated with 10% donkey serum before the addition of the antibodies as previously described (30). CD1d molecules were labeled with biotinylated antibody (BD Pharmingen, San Diego, CA), followed by streptavidin conjugated to Texas Red (Jackson ImmunoResearch, West Grove, PA). The immunofluorescently labeled cells were analyzed with a Bio-Rad MRC 1024 ES laser scanning confocal microscope and the $\times 60$ objective lens.
32. Gal(α 1-2)GalCer-dependent IL-4 production by splenocytes was reduced 20-fold by DGJ treatment.
33. We thank R. Molyneux from the USDA Western Regional Research Center in Albany, CA, for the gift of calystegine C1. We also thank L. Gapin and J. Matsuda for critical reading of the manuscript and S. Levery, J. Backstrom, and C. Benedict for helpful discussions. This work was supported by NIH grants AI40617 and CA52511 to M.K. and a Career Development Award from the Crohn's and Colitis Foundation of America to D.E. This is manuscript number 381 of the La Jolla Institute for Allergy and Immunology.

25 July 2000; accepted 15 December 2000

Nucleotide-Dependent Single-to Double-Headed Binding of Kinesin

Kenji Kawaguchi¹ and Shin'ichi Ishiwata^{1,2,3,4*}

The motility of kinesin motors is explained by a "hand-over-hand" model in which two heads of kinesin alternately repeat single-headed and double-headed binding with a microtubule. To investigate the binding mode of kinesin at the key nucleotide states during adenosine 5'-triphosphate (ATP) hydrolysis, we measured the mechanical properties of a single kinesin-microtubule complex by applying an external load with optical tweezers. Both the unbinding force and the elastic modulus in solutions containing AMP-PNP (an ATP analog) were twice the value of those in nucleotide-free solution or in the presence of both AMP-PNP and adenosine 5'-diphosphate. Thus, kinesin binds through two heads in the former and one head in the latter two states, which supports a major prediction of the hand-over-hand model.

Kinesin is a molecular motor that transports membrane-bound vesicles and organelles toward the plus end of a microtubule in various cells including neurons (1, 2). Kinesin takes hundreds of 8-nm steps (the size of tubulin heterodimers composed of α and β subunits) (3–5) before detachment, so that the run length reaches longer than 1 μ m (3, 6). Each step is associated with one cycle of ATP hydrolysis (7, 8). Structural and biophysical

evidence shows that stepping of kinesin is triggered by conformational changes in the ATP-bound head (9).

A "hand-over-hand" model has been proposed to explain the processive movement of kinesin (Fig. 1) (5, 9–16). To substantiate the hand-over-hand model, it is essential to determine the binding mode—either single- or double-headed binding—at each nucleotide state, and the kinetic step at which the transi-